

COMPARISON AMONG ROSIN *ET AL.*, HIGH FLOW STAIRMAND AND HIGH EFFICIENCY STAIRMAND CYCLONES CALCULATION METHODS

Marcelo José Pirani, pirani@unifei.edu.br

Rogério José da Silva, rogeriojs@unifei.edu.br

Manuel da Silva Valente de Almeida, msvalmeida@hotmail.com

Universidade Federal de Itajubá – UNIFEI, Av. BPS, 1303, bairro Pinheirinho, Itajubá – MG, CEP: 37500 903

Abstract. *The cyclones have application in several types of industries, as much as in processes in them developed, as integral part in systems for materials transportation, or still, as element of environmental pollution control. The variation of the constructive relationships and of the operation conditions of the cyclones, change your behavior, becoming essential for a good project, the knowledge of the variables that interfere in this operation. Thus, becomes important the accomplishment of a comparison among calculation methods of cyclones available in the literature. This work presents a comparison among the methods of Rosin et al., High Flow Stairmand and High Efficiency Stairmand for the determination of the separation efficiency and for the determination of pressure drop in cyclones. A granular distribution, by weight, of the particles to be separated in the cyclone is adopted and the separation efficiency and the pressure drop, using the proposed methods, are determined and discussed.*

Keywords: *cyclones, separation efficiency, pressure drop, calculation methods.*

1. INTRODUCTION

Cyclones or centrifugal collectors are devices used in industry to collect particles suspended in fluid flow through the centrifugal force. Fig. 1 shows a typical cyclone. Cyclones are used in various types of industries, either in the processes developed in them, either as part of methods for transporting materials, or as part of environmental pollution control, preventing emission of particulate materials to the atmospheric air.

Varella *et al.* (1987), cites applications of cyclones in industrial ventilation systems, removal of solid pollutants of the gas in boilers and furnaces, pneumatic conveying lines for separation of compressed airborne particles and in the cement industry as pre-calciner.

Mesquita *et al.* (1977), lists a number of industrial processes that use cyclones or multicyclones in coal mines, smelters, steel mills, among others. Nebra (1985), examined the use of cyclones in the drying of sugar cane bagasse, with the aim of improving efficiency in the burning of this product in sugar and alcohol plants.

The main advantages in application of cyclones are low cost, simplicity of design, construction and maintenance and ability to work with fluids at high temperature. Its main disadvantages are related to low efficiency in removing particles smaller than 5 μm and excessive abrasion to certain particles.

Vander Kolk *apud* Svanda (1967), makes the following points regarding the separation of particles by cyclones:

- Particles with diameter larger than 20 μm are easily separated by a good cyclone;
- Particles with diameter between 5 and 20 μm , the quality of the cyclone is fundamental;
- Particles with diameter between 2 and 5 μm , it is necessary a cyclone of exceptional quality to make the separation;
- Particles with diameter less than 2 μm are virtually impossible to separate them with reasonable efficiency even using the best cyclones.

2. OPERATING PRINCIPLE

The operating principle of a cyclone is based on the centrifugal force acting on the particles carried by the gas. The gas, which is usually the air, together with the particles to be separated, enters the cyclone tangentially at the top, creating a downward spiral flow between the wall and the outlet duct, this spiral is called the primary spiral and extends through the base of cone. The spiral movement creates centrifugal force acting on the particles and is several times greater than the force of gravity, dragging these particles toward the walls, removing them of the flow of gas through the bottom of the cyclone. The gas then, free of particles, returns in upward spiral movement through the cyclone center to the exit duct. The spiral formed by the upward spiral movement is called secondary spiral.

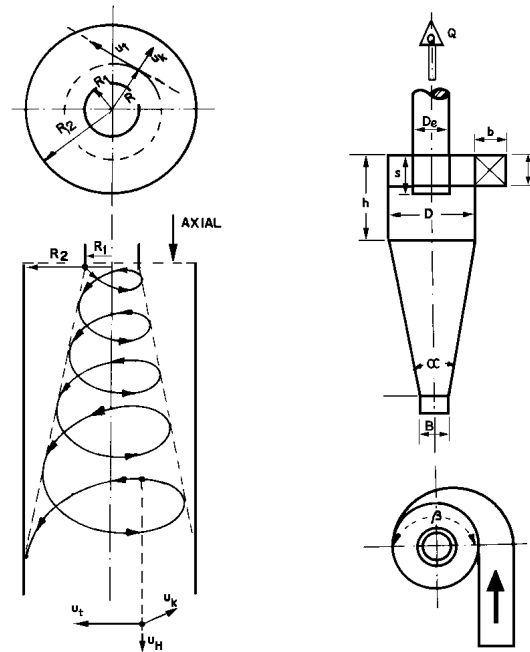


Figure 1. Scheme of a typical cyclone

3. MODELS FOR DETERMINATION OF EFFICIENCY AND PRESSURE DROP IN CYCLONES

3.1. Rosin *et al.* Model

One way to determine the separation efficiency of a cyclone is through the "cut diameter" of the cyclone, which corresponds to the particle size for which is obtained 50% efficiency of separation. The cut diameter of the cyclone, according to Rosin *et al.* *apud* Perry (1973) is given by Eq. 1, as follows:

$$d_{50} = 3 \sqrt{\frac{\mu b}{\pi (\rho_p - \rho) N U_i} \left(1 - \frac{2b}{D}\right)} \quad (1)$$

where a is the height and b is the width of the intake duct of the cyclone (Fig. 1), μ is the dynamic viscosity of carrier gas, which is usually the air, ρ is the density of carrier gas, ρ_p is density of the particle, N is the number of turns that particle gives in the cyclone before being collected ($N = 5$ for Rosin model), U_i is the gas flow velocity at the inlet of cyclone and D is the diameter of the cyclone (Fig. 1).

For the case where the carrier gas is the air, the density can be determined using the ideal gas equation and the dynamic viscosity can be determined using the equation of Sutherland *apud* Silva *et al.* (2010), given by:

$$\mu_{ar} = \frac{1.458 \times 10^{-6} \times T^{1/2}}{1 + 110.4/T} \quad (2)$$

where temperature, T must be in Kelvin for the dynamic viscosity, μ_{ar} in Pa.s.

This model assumes that a particle spinning in a circle where there is the maximum tangential velocity has a 50% chance of being collected. To continue turning in this circle the movement of particles toward the wall of the cyclone must be balanced by the drag of the gas flowing toward the geometric center of the cyclone.

From the results obtained with Eq. 1 and after conducting several experiments, Rosin *et al.* *apud* Perry (1973), constructed the graph shown in Fig. 2, which in essence is a generalized form of the graph of fractional efficiency often found in commercial literature. For cyclone proportions as shown in Fig. 2, the value of N that appears in Eq. 1 is around 5.

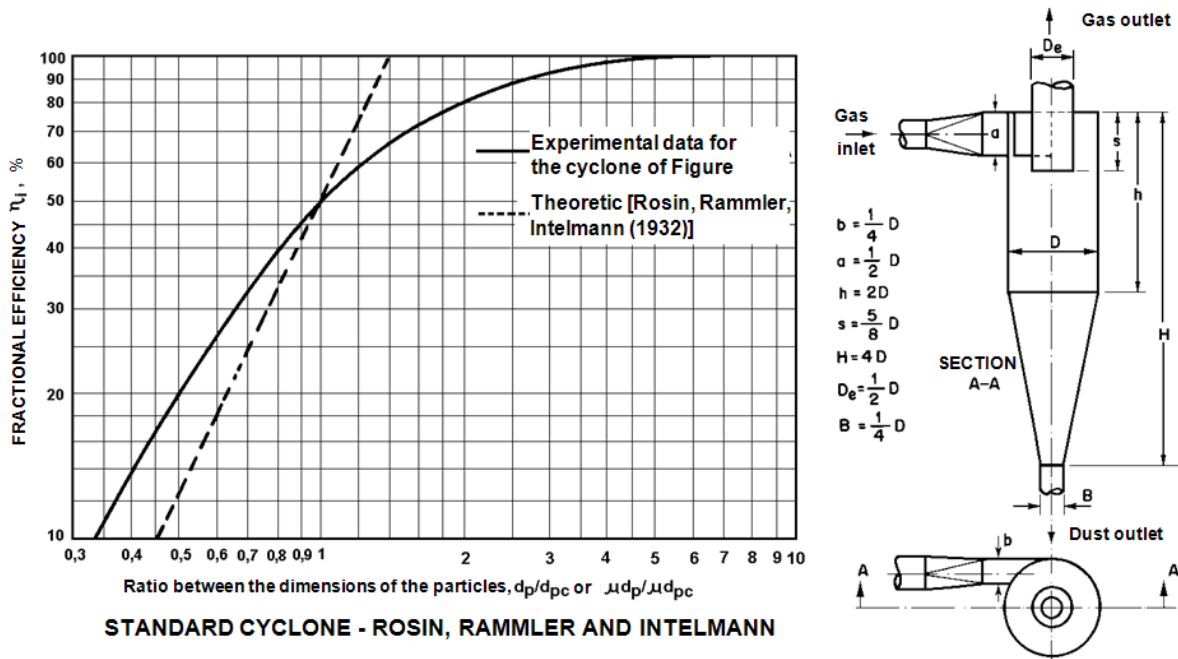


Figure 2. Standard Cyclone - Rosin, and Raimmler Intelmann.

The expression for the determination of pressure drop in Rosin *et al.* cyclone, according to Perry (1973), is given by:

$$\Delta P = \frac{8.0 \rho U_i^2}{2g} \quad [\text{mmH}_2\text{O}] \quad (3)$$

where g is the gravity acceleration .

The pressure drop can also be determined using the expression developed by Casal and Martinez-Benet *apud* Silva *et al.* (2010), given by Eq. 4.

$$\Delta P = \rho \frac{U_i^2}{2g} \left[11.3 + \left(\frac{ab}{D_e} \right)^2 + 3.33 \right] \quad [\text{mmH}_2\text{O}] \quad (4)$$

where D_e is the diameter of the gas outlet duct of the cyclone.

3.2. High flow and high efficiency Stairmand Models.

According to Stairmand (1951), if the frictional force of the fluid on the particle can be represented by Stokes law, and if the average radial velocity U_R is balanced by the centrifugal force on the particle, then the cut diameter can be determined through of Eq. 5.

$$d_{50} = \frac{3}{\psi U_i} \sqrt{\frac{\dot{Q} \mu D_e}{2\pi \rho_p - \rho H - S D}} \quad (5)$$

where, according to Figures 3 and 4, H is the total height of the cyclone, S is the length of the outlet duct, that is within the cyclone, \dot{Q} is the flow rate through the cyclone, and ψ is the friction factor in the cyclone walls defined by Eq. 6:

$$\psi = \frac{-\left(\frac{D_e}{2D-b}\right)^{1/2} + \left(\frac{D_e}{2D-b} + \frac{4GA}{ab}\right)^{1/2}}{2GA/ab} \quad (6)$$

where G is the dimensionless constant of friction loss of Stanton and Pannell *apud* Silva *et al.* (2010), equal to 0.005 for gas cyclones and A is the cyclone surface area exposed to the gases, given by Eq. 7.

$$A = \pi Dh + 2\pi D_e S + \pi \left(\frac{B+D}{2}\right) \left[H - h^2 + \left(\frac{D+B}{2}\right)^2 \right]^{1/2} + \pi \left(\frac{D^2 - D_e^2}{4}\right) \quad (7)$$

where, according to Figures 3 and 4, h is the height of the cylindrical part of cyclone, B is the diameter of the exit duct of particles from the cyclone.

Stairmand (1951), obtained experimental curves of fractional efficiency for two families of cyclones, a medium-efficiency and high flow, as shown in Fig. 3 and a high separation efficiency and low flow, as shown in Fig. 4.

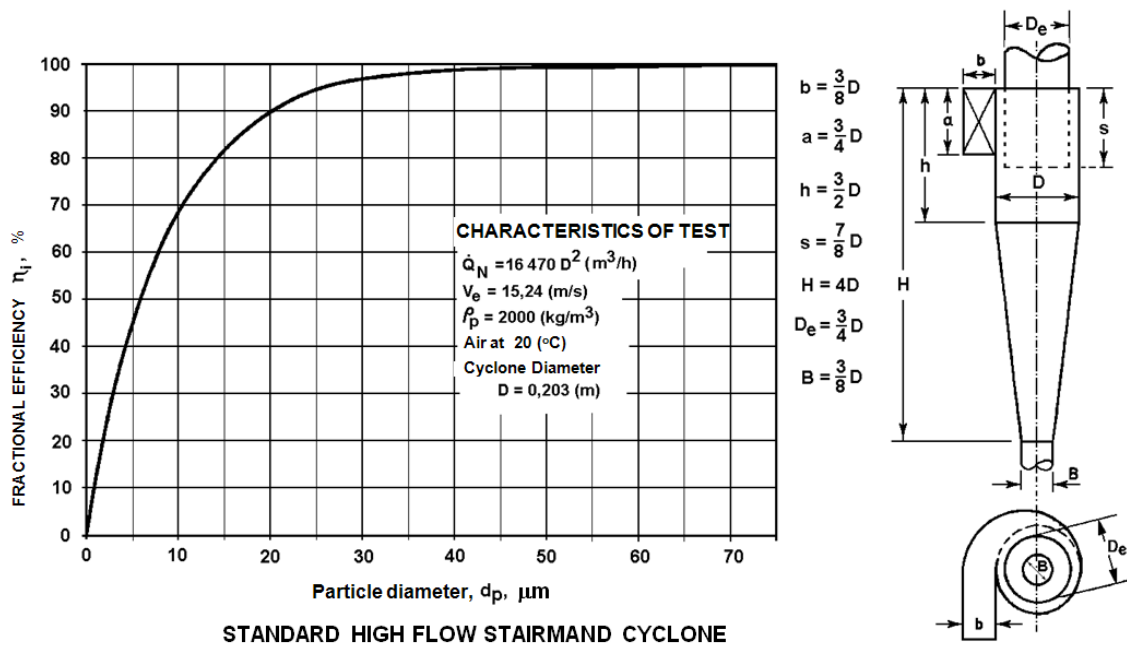


Figure 3. Standard High-Flow Stairmand Cyclone.

These curves tend to confirm the experimental data of Ter Linden (1949), in that relatively longer cyclones with smaller output duct diameter are more efficient than cyclone with bigger output duct diameter and relatively shorter shape.

According to Stairmand (1951), the efficiency of cyclones of the same family (built with the same proportions) operating under conditions different of the test conditions can be determined by similarity through its respective cut diameter model, ie:

$$\left(\frac{\bar{d}_p}{d_{p,Teste}}\right)_{\eta_i,Teste} = \left[\left(\frac{\rho_{Teste}}{\rho_p}\right) \times \left(\frac{\mu}{\mu_{Teste}}\right) \times \left(\frac{U_{i,Teste}}{U_i}\right) \times \left(\frac{D}{D_{Teste}}\right) \right]^{1/2} \quad (8)$$

where \bar{d}_p is the average diameter of particles to be collected, $d_{p,Teste}$, $U_{i,Teste}$, ρ_{Teste} , D_{Teste} e μ_{Teste} are the values used in experimental tests of Stairmand (1951), defined as: $d_{p,Teste}$ is the diameter of the particles, which corresponds to the abscissa axis in Figures 3 and 4, $U_{i,Teste}$ is the gas velocity at the cyclone entry equal to 15.24 m/s, ρ_{Teste} is the specific gravity equal to 2000 kg/m³, D_{Teste} is the cyclone diameter equal to 0.203 m and μ_{Teste} is the dynamic viscosity of the air determined through Eq. 2 using a temperature of 20°C (293K) which is the temperature of the tests.

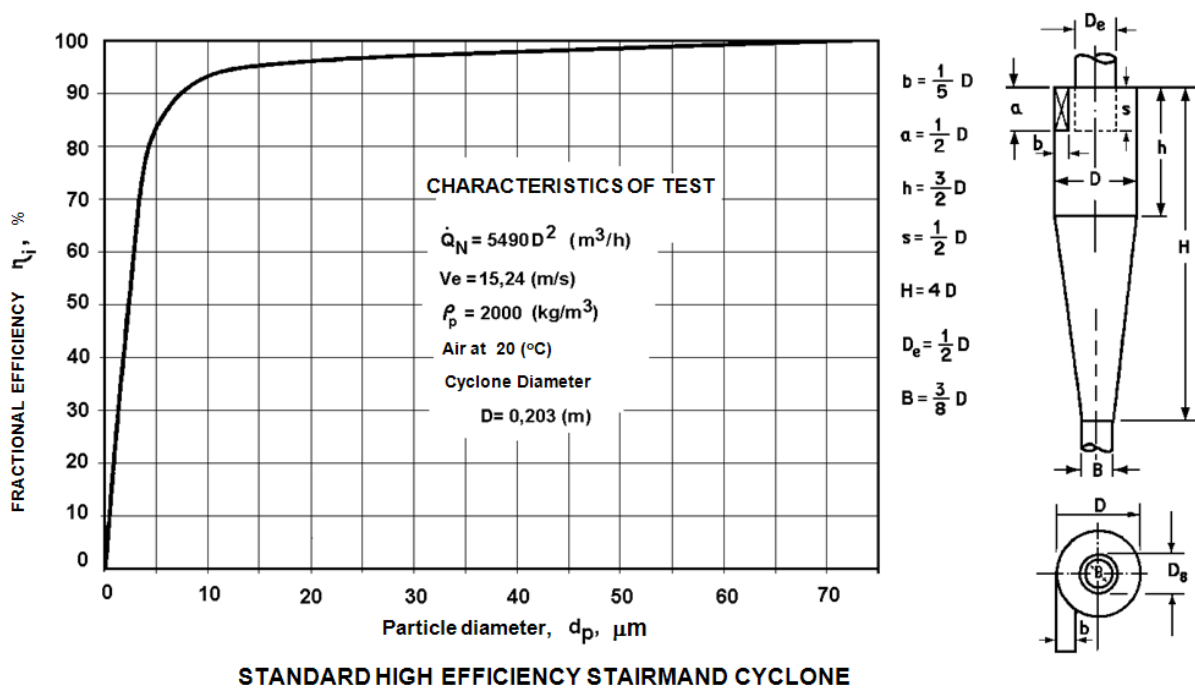


Figura 4. Standard High Efficiency Stairmand Cyclone.

Equation 8 can be used to determine the fractional and overall separation efficiency of the cyclone built with the same geometric proportions of the cyclone that efficiency curves were obtained experimentally. Figures 3 and 4 show, respectively, the experimental curves obtained for the cyclones families of high flow and high efficiency Stairmand.

The expression for determining the pressure drop, according to Stairmand (1951), is given by:

$$\Delta P = \frac{\rho + \rho'_p}{2g} \left\{ U_i^2 \left[1 + 2\psi^2 \left(\frac{2D-b}{D_e} - 1 \right) \right] + 2U_s^2 \right\} \quad [\text{mmH}_2\text{O}] \quad (9)$$

where ρ'_p can be calculated as:

$$\rho'_p = C_o \rho_p - \rho \quad (10)$$

where C_o is the concentration of particles in the flow, given by:

$$C_o = \frac{\dot{m}_p / \rho_p}{\dot{m}_p / \rho_p + \dot{m}_f / \rho_f} \quad (11)$$

ψ is the friction factor calculated by Eq. 6 and U_s is the gas velocity at the exit of the cyclone, calculated as:

$$U_s = \frac{4 \times \dot{Q}}{\pi \times D_e^2} \quad (12)$$

In Eq. 11 the mass amount of particles entering the cyclone \dot{m}_p per unit time can be determined by the following expression:

$$\dot{m}_p = \dot{M}_p \times \dot{Q} \quad (13)$$

where \dot{M}_p is the mass of particles entering the cyclone per cubic meter of gas.

The mass flow of air that appears in Eq. 11 can be determined by the following expression:

$$\dot{m}_f = \dot{Q} \times \rho \tag{14}$$

The expression for determining the pressure drop developed by Casal and Martinez-Benet, *apud* Silva *et al.* (2010), Eq. 4, can also be used in Stairmand cyclones of high flow and high efficiency.

3. APPLICATION

To illustrate the methodology used, in this item is presented the calculation of the fractional efficiency and of the pressure drop using the models of Rosin *et al.*, high flow Starmaind and high efficiency Starmaind. To enable the calculations will be used data from a local exhaust ventilation system of a hypothetical carpentry. Data are presented in Tab. 1. The distribution of particles in function of diameter and also the weight percentage corresponding for each range of particle size are presented in Tab. 2

Table 1. Data from local exhaust ventilation system to be analyzed

Volumetric flow rate of air, \dot{Q} [m ³ /s]	1.024
Air velocity at the entrance of the cyclone, U_i [m/s]	10
Material to be separated	Wood
Wood specific gravity, ρ_p [kg/m ³]	510
Local atmospheric pressure, P_{atm} [Pa]	101325
Process temperature, T [°C]	30
Mass quantity of particles entering the cyclone per cubic meter of gas \dot{M}_p [kg of wood / m ³ of air]	0.012

Table 2. Particle size distribution

Particle size distribution, where d_p is the particle diameter [µm]	Average particle diameter \bar{d}_p (adopted) [µm]	Percentage by weight (% P) in each particle size range
$d_p > 160$	160	50%
$120 < d_p \leq 160$	140	30%
$40 < d_p \leq 120$	80	15%
$d_p \leq 40$	20	5%
Total		100%

- Determination of cyclones dimensions

To determine the dimensions of the cyclone, first is estimated the diameter D through the Eq. 15 shown following:

$$\dot{Q} = a \times b \times U_i \tag{15}$$

With the values of \dot{Q} and U_i known and with the expressions of a and b from Figures 2, 3 or 4, depending on the model, the diameter D is determined. For the model of Rosin *et al.*, for example, the expressions for a and b are, respectively, $a=D/2$ and $b=D/4$.

Table 3 shows the dimensions of cyclones for the three models used.

Table 3. Cyclones Dimensions.

MODEL	DIMENSIONS [m]							
	D	a	b	h	s	H	D _e	B
Rosin <i>et al.</i>	0.905	0.453	0.226	1.810	0.566	3.620	0.453	0.226
High-flow Stairmand	0.603	0.453	0.226	0.905	0.528	2.414	0.453	0.226
High efficiency Stairmand	1.012	0.506	0.202	1.518	0.506	4.048	0.506	0.379

3.1 Rosin *et al.* Model

- Determination of cut diameter according to Rosin *et al.* model *apud* Perry (1973).

The cut diameter according to Rosin *et al.* model is determined from Eq. 1, resulting in:

$$d_{50} = 1.539 \times 10^{-5} \text{ m}$$

- Determination of fractional and total efficiency according to Rosin *et al.* model *apud* Perry (1973).

Considering the particle size distribution presented in Tab. 2 and the cut diameter d_{50} calculated by Eq. 1, the value of \bar{d}_p / d_{50} is obtained. Entering with values of \bar{d}_p / d_{50} in Fig. 2, the fractional efficiency and consequently the overall efficiency is determined, as shown in Tab. 4.

Table 4. Fractional efficiency η and total efficiency η_T according to Rosin *et al.* model *apud* Perry (1973).

\bar{d}_p [μm] adopted	\bar{d}_p / d_{50}	η_i [%]	$\%P_i$ [%]	$\eta_i \times \%P_i / 100$
160	10.3	100.0	50	50.0
140	9.0	100.0	30	30.0
80	5.2	98.0	15	14.7
20	1.3	63.0	5	3.1
Total			100%	$\eta_T = 97.8$

- Determination of pressure drop according to Rosin *et al.* model *apud* Perry (1973).

The pressure drop according to Rosin *et al.* model *apud* Perry (1973) is determined by Eq. 3, resulting in:

$$\Delta P = 47.5 \text{ mmH}_2\text{O}$$

3.2 High flow Stairmand Model.

- Determination of the cut diameter according to high flow Stairmand model.

Applying the similarity method (Eq. 8) to determine the efficiency of the cyclone and considering Fig. 3, results:

$$\left(\frac{\bar{d}_p}{d_{p,Teste}} \right)_{n_i,Teste} = 4.3 \text{ or} \tag{16}$$

$$d_{p,Teste} = \frac{\bar{d}_p}{4.3} \quad (17)$$

- Determination of fractional and total efficiency according to high flow Stairmand model.

Considering the particle size distribution presented in Tab. 2 and determining the diameter $d_{p,Teste}$ by Eq. 17, the value of fractional efficiency $\eta_{i,Teste}$ is obtained from Fig. 3, resulting in the Tab. 5, following:

Table 5. Fractional efficiency $\eta_{i,Teste}$ and total efficiency η_T according to high flow Stairmand model.

\bar{d}_p (μm) adopted	$d_{p,Teste}$	$\eta_{i,Teste}$ [%]	$\%P_i$ [%]	$\eta_i \times \%P_i / 100$
160	37.2	98.0	50	49.0
140	32.6	98.0	30	29.4
80	18.6	88.0	15	13.2
20	4.6	40.0	5	2.0
Total			100%	$\eta_T = 93.6$

- Determination of pressure drop according to high flow Stairmand model.

Using Eq.s 6, 7, 9, 10, 11 and 12 for the determination of pressure drop, results:

$$\Delta P = 18.22 \text{ mmH}_2\text{O}$$

3.3 High efficiency Stairmand Model.

- Determination of the cut diameter according to high efficiency Stairmand model.

Similarly to high flow Stairmand model, results:

$$d_{p,Teste} = \frac{\bar{d}_p}{5.4} \quad (18)$$

- Determination of fractional and total efficiency according to high efficiency Stairmand model.

Considering the particle size distribution presented in Tab. 2 and determining the diameter $d_{p,Teste}$ by Eq. 18, the value of fractional efficiency $\eta_{i,Teste}$ is obtained from Fig. 4, resulting in the Tab. 6, following:

Table 6. Fractional efficiency $\eta_{i,Teste}$ and total efficiency η_T according to high efficiency Stairmand model.

\bar{d}_p (μm) adopted	$d_{p,Teste}$	$\eta_{i,Teste}$ [%]	$\%P_i$ [%]	$\eta_i \times \%P_i / 100$
160	28.9	97.0	50	48.5
140	25.3	96.5	30	29.0
80	14.5	95.0	15	14.2
20	3.6	80.0	5	4.0
Total			100%	$\eta_T = 95.7$

- Determination of pressure drop according to high efficiency Stairmand model.

Using Eq.s 6, 7, 9, 10, 11 and 12 for the determination of pressure drop, results:

$$\Delta P = 30.27 \text{ mmH}_2\text{O}$$

3.4 Results for the overall efficiency and pressure drop.

Table 7 shows the values of cyclone efficiency in terms of inlet velocity for the three models used, and Fig. 5 shows the graph corresponding to Tab. 7.

Table 7. Efficiency of the cyclone in terms of inlet velocity.

Inlet Velocity U_i	Total efficiency of the cyclone η_T		
	Rosin <i>et al.</i>	High Flow Stairmand Model	High Efficiency Stairmand Model
6.0	96.0	86.8	92.7
8.0	97.4	92.3	93.9
10.0	97.8	93.6	95.7
12.0	98.1	94.8	96.1
14.0	98.6	95.5	96.1
16.0	98.9	96.2	96.7

Table 8 shows the values of pressure drop in the cyclone in terms of inlet velocity for the three models used, and Fig. 6 shows the graph corresponding to Tab. 8.

Table 8. Pressure drop in the cyclone in terms of inlet velocity.

Inlet Velocity U_i	Pressure drop in the cyclone $\Delta P [mmH_2O]$		
	Rosin <i>et al.</i>	High Flow Stairmand Model	High Efficiency Stairmand Model
6.0	17.1	6.6	10.8
8.0	30.4	11.7	19.2
10.0	47.5	18.2	30.3
12.0	68.4	26.2	43.1
14.0	93.1	35.7	58.7
16.0	121.6	46.6	76.7

It is observed on the graph shown in Fig. 5 that the Rosin *et al.* cyclone model has the highest efficiency among the three models and high flow Stairmand model has the lowest efficiency. It was also noted that efficiency increases with increasing of velocity in the entrance of the cyclone, confirming the experimental results obtained by Ter Linden (1949).

It should be noted that the cyclone of Rosin *et al.* presents highest efficient, but also presents highest pressure drop, as can be seen in Fig. 6. In Fig. 6 is also possible to see that the pressure drop increases with increasing of velocity in the entrance of the cyclone, again confirming the experimental results obtained by Ter Linden (1949). Increasing the velocity in the entrance can lead to extremely high pressure drops, which is why, in the design of cyclones, the velocity usually used, according to Perry (2004), is 15m/s.

According to Ter Linden (1949), increasing the diameter D of the cyclone in respect to the diameter of the exit duct results in increased efficiency, in fact, comparing the dimensions of the cyclones of Rosin *et al.* and high efficiency Stairmand, shown in Tab. 3, with the high flow Stairmand cyclone, it is observed that the first two show the ratio of D/D_e , greater than the value for the high flow Stairmand cyclone, and consequently greater efficiency.

4. CONCLUSIONS

Based on obtained results it is observed that different families of cyclones have different values for the efficiency and different values for the pressure drop, even if the particle size distribution is identical.

For a cyclone already installed, if it is necessary to increase the efficiency without changing its geometry, may be increased the velocity at the entrance of the cyclone, remembering that the pressure drop will increase. This tendency can be observed in Figures 5 and 6.

The efficiency and pressure drop influence the cost of installation and operating cost, which should always be considered when choosing the optimal cyclone for a particular application.

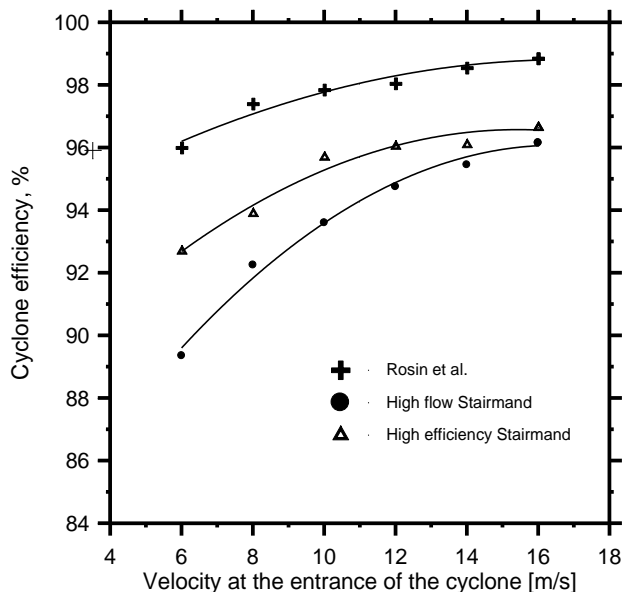


Figure 5. Efficiency of the cyclone in function of velocity at the entrance.

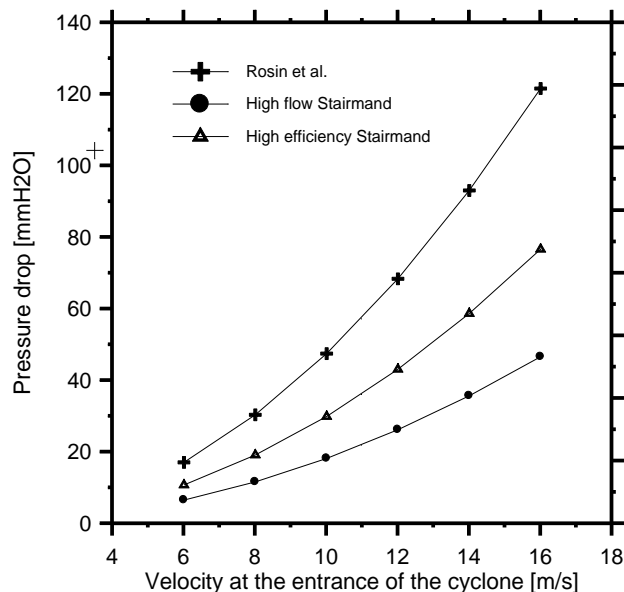


Figure 6. Pressure drop of the cyclone in function of velocity at the entrance.

5. REFERENCES

- Mesquita, A.L.S., Guimarães, F.A., Nefussi, N., 1977, “Engenharia de Ventilação Industrial”, Editora Edgard Blucher Ltda.
- Nebra, S.A., 1985, “Secagem Pneumática de Bagaco de Cana”, Tese de Doutorado, Universidade Estadual de Campinas, Campinas, Brasil.
- Perry, R.H., Chilton, C.H., 1973, “Chemical Engineers Handbook”. International Student Edition, Fifth edition, section 20.
- Perry, R.H., Green, D.W., 1997, “Perry’s Chemical Engineers’ Handbook”. Seventh Edition, Ed. McGraw Hill.
- Sairmand, C.J., 1951, “The Design and Performance of Cyclones Separators”, Trans. Instn. Chem. Engrs, Vol. 29, pp. 356 to 383.
- Silva, E., Almeida, M.S.V., Varella, S., 2010, “Ventilação Industrial”, Apostila da Fundação de Pesquisa e Assessoramento à Indústria – FUPAI, Itajubá, Minas Gerais, Brasil.
- Svanda, J., 1967, “Cyclone Calculations and some Design Parameters Affecting Cyclone Efficiency”, Internatinal Chemical Engineering, Vol. 7, pp. 238 to 245.
- Ter Linden, A.J., 1949, “Investigation into cyclone dust collectors”. Proceedings of the institution of mech. Eng. J., Vol. 160, pp. 233-251.
- Varella, S., Silva, E., Silva, R.J., 1987, “Desempenho de Ciclones. Uma Avaliação Teórica Experimental”, Congresso Brasileiro de Engenharia Mecânica (COBEM), 1987, Florianópolis, Brasil.

6. RESPONSIBILITY NOTICE

The authors are the only responsible for the printed material included in this paper.